Biogeosciences Discuss., https://doi.org/10.5194/bg-2019-143
Manuscript under review for journal Biogeosciences
Discussion started: 26 April 2019

Biogeosciences Discussions Open Access EGU

Vertical partitioning of CO_2 production in a Dystric Cambisol

Patrick Wordell-Dietrich[1,2], Axel Don[2], Anja Wotte[3,4], Janet Rethemeyer[4], Jörg Bachmann[5], Mirjam Helfrich[2], Kristina Kirfel[6], and Christoph Leuschner[6]

[1]Institute of Soil Science and Site Ecology, Technische Universität Dresden, Pienner Straße 19, 01737 Tharandt, Germany
[2]Thünen Institute of Climate-Smart Agriculture, Bundesallee 50, 38116 Braunschweig, Germany
[3]Institute of Geology, Technische Univesität Bergakademie Freiberg, Bernhard-von-Cotta Straße 2, 09599 Freiberg, Germany
[4]Institute of Geology and Mineralogy, University of Cologne, Zülpicher Straße 49b, 50674 Köln, Germany
[5]Institute of Soil Science, Leibniz University Hannover, Herrenhäuser Straße 2, 30451 Hannover, Germany
[6]Plant Ecology, Albrecht Haller Institute for Plant Science, University of Göttingen, Untere Karspüle 2, 37073 Göttingen, Germany

Correspondence: Patrick Wordell-Dietrich (patrick.wordell-dietrich@tu-dresden.de)

Abstract. Large amounts of total organic carbon are temporarily stored in soils, which makes soil respiration one of the major sources of terrestrial CO_2 fluxes within the global carbon cycle. More than half of global soil organic carbon (SOC) is stored in subsoils (below 30 cm), which represent a significant C pool. Although several studies and models have investigated soil respiration, little is known about the quantitative contribution of subsoils to total soil respiration or about the sources of CO_2 production in subsoils. In a two-year field study in a European beech forest in northern Germany, vertical CO_2 concentration profiles were continuously measured at three locations and CO_2 production quantified in the topsoil and the subsoil. To determine the contribution of fresh litter-derived C to CO_2 production in the three soil profiles, an isotopic labelling experiment using ^{13}C-enriched leaf litter was performed. Additionally, radiocarbon measurements of CO_2 in the soil atmosphere were used to obtain information about the age of the C source in CO_2 production. At the study site, it was found that 90 % of total soil respiration was produced in the first 30 cm of the soil profile where 53 % of the SOC stock is stored. Freshly labelled litter inputs in the form of dissolved organic matter were only a minor source for CO_2 production below a depth of 10 cm. In the first two months after litter application, fresh litter-derived C contributed on average 1 % at 10 cm depth and 0.1 % at 150 cm depth to CO_2 in the soil profile. Thereafter, its contribution was less than 0.3 % and 0.05 % at 10 cm and 150 cm depths respectively. Furthermore CO_2 in the soil profile had the same modern radiocarbon signature at all depths, indicating that CO_2 in the subsoil originated from young C sources, despite a radiocarbon age bulk SOC in the subsoil. This suggests that fresh C inputs in subsoils in the form of roots and root exudates are rapidly respired and that other subsoil SOC seems to be relatively stable. The field labelling experiment also revealed a downward diffusion of $^{13}CO_2$ in the soil profile against the total CO_2 gradient. This isotopic dependency should be taken into account when using labelled $^{13}CO_2$ and ^{14}C isotope data as an age proxy for CO_2 sources in the soil.

Biogeosciences Discuss., https://doi.org/10.5194/bg-2019-143
Manuscript under review for journal Biogeosciences
Discussion started: 26 April 2019

1 Introduction

Soils are the world's largest terrestrial organic carbon (C) pool, with an estimated global C stock of about 2400 Gt in first two metres of the world's soils (Batjes, 2014). The CO_2 efflux from soils, known as soil respiration, is the second largest flux component in the global C cycle (Bond-Lamberty and Thomson, 2010; Raich and Potter, 1995) and can be divided into autotrophic respiration due to roots black and mycorrhizae and heterotrophic respiration due to mineralization of soil organic carbon (SOC) by decomposers. Global warming is expected to increase soil respiration by boosting the microbial decomposition of SOC (Bond-Lamberty et al., 2018; Hashimoto et al., 2015) and by greater root respiration (Schindlbacher et al., 2009; Suseela and Dukes, 2013). Although most of the CO_2 is produced in topsoils (< 30 cm), a significant amount of CO_2 is produced in the subsoil (> 30 cm) (Davidson and Trumbore, 1995; Drewitt et al., 2005; Fierer et al., 2005; Jassal et al., 2005). Despite the fact that more than 50 % of global SOC stocks are stored in subsoils (Batjes, 2014; Jobbágy and Jackson, 2000), little is known about the amount and sources of CO_2 production in subsoils. Moreover, the mechanisms controlling CO_2 production in subsoils are still not fully understood. High apparent radiocarbon (^{14}C) ages of SOC in subsoils (Rethemeyer et al., 2005; Torn et al., 1997) lead to an assumption of a high stability of C and a low turnover in subsoils. However, laboratory incubations of subsoil samples show similar mineralisation rates of SOC in both subsoils and topsoils (Agnelli et al., 2004; Salomé et al., 2010; Wordell-Dietrich et al., 2017), suggesting that subsoils also contain a labile fraction that should be taken into account as a source for soil respiration.

A range of studies have been conducted on CO_2 production in soils, but most of them have focused on spatial variations in temperature, water content and substrate supply (Borken et al., 2002; Davidson et al., 1998; Fang and Moncrieff, 2001), but ignoring the vertical partitioning of CO_2 production in the whole soil profile which is essential for understanding soil C dynamics. One reason for this might be the measurement methods used to quantify sources and fluxes in the soil profile. Total CO_2 production can easily be measured at the soil surface with an open-bottom chamber, whereas vertical monitoring of CO_2 production needs determination of CO_2 concentrations at several soil depths in order to estimate CO_2 production, i.e. using the gradient method first described by de Jong, E., Schappert (1972). Basically, the CO_2 flux between two depths can be calculated using the effective gas diffusion coefficient and the CO_2 gradient between the two depths. Recently, the development of low-cost sensors for temperature, soil moisture and CO_2 concentration has allowed greater use of the gradient method (Jassal et al., 2005; Maier and Schack-Kirchner, 2014; Pingintha et al., 2010; Tang et al., 2005). This method can help quantify CO_2 production in the entire soil profile, which is essential for an improved quantitative understanding of whole soil C dynamics including the important contribution made by subsoil. To date there have only been a few studies that have continuously determined CO_2 production in the whole soil profile *in situ* over a longer timescale (Goffin et al., 2014; Moyes and Bowling, 2012).

In the present study, the vertical distribution of CO_2 concentration was measured and CO_2 production rates calculated over a two-year period in a Dystric Cambisol in a temperate beech forest. The objectives of this study were 1) to quantify the contribution of CO_2 production in subsoils to total soil CO_2 production, and 2) to identify sources of CO_2 production along the

Biogeosciences Discuss., https://doi.org/10.5194/bg-2019-143
Manuscript under review for journal Biogeosciences
Discussion started: 26 April 2019

soil profile using sources partitioning *via* isotopic data (^{13}C and ^{14}C). It was hypothesised that the majority of CO_2 in subsoils originates from young C sources and not from mineralisation of old SOC.

2 Methods

2.1 Site description and subsoil observatories

The study site is located in a beech forest (Grinderwald) 35 km northwest of Hannover, Germany (52°34´22´´N, 9°18´49´´E). The vegetation is dominated by common beech trees (*Fagus sylvatica*) that were planted in 1916 and the soil is characterised as a Dystric Cambisol (IUSS Working Group WRB, 2014) developed on Pleistocene fluvial and aeolian sandy deposits from the Saale glaciation. The site is located around 100 m above sea level, with a mean annual temperature and precipitation of 9.7 °C and 762 mm (1981–2010) respectively. The soil texture of the site is mainly composed of the sand fraction with contents varying from 60 % (< 30 cm) to 90 % (> 120 cm), with SOC contents of 11.5 g kg^{-1} down to (10 cm) 0.4 g kg^{-1} (185 cm) (Heinze et al., 2018; Leinemann et al., 2016).

In July 2013, three subsoil observatories were installed using a stainless steel lysimeter vessel (1.6 m diameter and 2 m height) driven 2 m deep into the soil. Once the vessel had been inserted, the soil inside the containment was excavated by hand and undisturbed soil cores (5.7 cm inner diameter, 4.0 cm height) taken with five replicates at depths of 10, 30, 50, 90 and 150 cm from each subsoil observatory for soil diffusivity measurements. In addition, undisturbed soil samples in the observatories were taken to estimate fine root density. Thus six samples were taken from the forest floor and six samples from each of the upper mineral soil layers (0–10 cm, 10–20 cm, 20–40 cm) using a soil corer (3.5 cm diameter), and three samples were taken from each depth increment of the lower profile (40–200 cm depth) at 20 cm depth intervals using a steel cylinder (12.3 cm diameter and 20 cm height). In the laboratory, the samples were gently washed over sieves of 0.25-mm mesh size to separate the roots from adhering soil particles. Under the stereo microscope, the rootlets were separated into live (biomass) and dead (necromass) roots, and subsequently into fine (< 2 mm in diameter) and coarse roots (> 2 mm in diameter). All live and dead root samples were dried at 70 °C for 48 h and weighed.

After the lysimeter vessel was removed, a polyethylene shaft (1.5 m in diameter and 2.1 m height) was placed in the soil, referred to here as the subsoil observatory. The gap (≈ 5 cm) between the subsoil observatory and the surrounding undisturbed soil was refilled. The observatories where installed close to one other, with a maximum distance of 30 m between them.

To monitor the temperature and volumetric water content, combined temperature and moisture sensors (UMP-1,Umwelt-Geräte-Technik GmbH, Germany) were installed at depths of 10, 30, 50, 90 and 150 cm with a horizontal distance of 100 cm from the wall of the subsoil observatories. Measurements were taken every 15 minutes and stored on a data logger. The CO_2 concentration in the soil air was monitored by solid-state infrared gas sensors (GMP221, Vaisala Oyi, Finland) with a measuring range of 0–10 % CO_2. To protect the PTFE membrane of the CO_2 sensor from damage while being placed in the soil, the sensor was coated with an additional PTFE foil (616.13 P, FIBERFLON, Turkey), to allow gaseous diffusion and prevent water infiltration. The CO_2 concentration was measured every three hours to reduce power consumption. The CO_2 sensors were turned on 15 minutes before the measurement itself due to their warm-up time. In addition, PTFE suction cups

Biogeosciences Discuss., https://doi.org/10.5194/bg-2019-143
Manuscript under review for journal Biogeosciences
Discussion started: 26 April 2019

for soil air sampling with stainless steel tubing (ecoTech Umwelt-Meßsysteme GmbH, Germany) were installed adjacent to the CO_2 sensors. The gas samplers and CO_2 sensors were installed at the same depths as the temperature and moisture sensors. The horizontal distance of the gas samplers and CO_2 sensors from the subsoil observatory wall increased from 40 cm to 100 cm with increasing soil depth.

2.2 Gas sampling and measurements

2.2.1 Soil respiration

The surface CO_2 efflux was measured using the closed-chamber method. Thirty PVC collars with a diameter of 10.4 cm and a height of 10 cm were installed 5 cm deep in the soil around the three subsoil observatories. The organic layer of 15 collars was removed in order to be able to distinguish between mineral soil respiration and total soil respiration. Soil respiration was measured with the EGM-3 SRC-1 soil respiration chamber (PP-Systems, USA) and the LI-6400-09 soil chamber (LI-COR Inc., USA). The measurement system was changed due to technical problems with the EGM-3 system, however a comparison between the two systems revealed only minor differences. Each collar was measured three times per sampling day from March 2014 to March 2016, with sampling ranging from once a month to once a week. Annual soil respiration was derived from linear interpolation of measured CO_2 fluxes from the collars. Furthermore, soil respiration was modelled by fitting an Arrhenius-type model (Eq.1), introduced by Lloyd and Taylor (1994) and using soil temperature data from 10 cm depth, and the measured CO_2 fluxes:

$$F_0 = a \times e^{\left(\frac{E_0}{T + 273.2 - T_0} \times \frac{T - 10}{283.2 - T_0}\right)} \quad (1)$$

where F_0 is soil respiration [µmol m^{-2} s^{-1}], a, E_0 and T_0 are fitted model parameters, and T is the soil temperature at 10 cm depth [°C].

2.2.2 $^{13}CO_2$ sampling and measurement

In addition to continuous CO_2 concentration monitoring, two gas samples per depth and subsoil observatory were taken from the suction cups with a syringe and filled into 12-mL evacuated gas vials (Labco Exetainer, Labco Limited, UK). The sampling started in May 2014 with an interval of between once a month and once a week. The CO_2 concentration in the soil gas samples was analysed by gas chromatography (Agilent 7890A, Agilent Technologies, USA). The $\delta^{13}C$ values of the CO_2 samples were measured by an isotope ratio mass spectrometer (Delta Plus with GP interface and GC-Box, Thermo Fisher Scientific, Germany) connected to a PAL autosampler (CTC Analytics, Switzerland). The ^{13}C results are expressed in parts per thousand (‰) relative to the international standard Vienna Pee Dee Belemnite (VPDB).

2.2.3 $^{14}CO_2$ sampling and measurement

Soil gas samples for radiocarbon analysis were taken in October and December 2014 in subsoil observatories 1 and 3. The CO_2 was sampled using a self-made molecular sieve cartridge as described in Wotte et al. (2017). Briefly, each stainless steel

cartridge was filled with 500 mg zeolite type 13X (40/60 mesh, Charge 5634, IVA Analysetechnik GmbH & Co KG, Germany), which is used as an adsorbent for CO_2. The molecular sieve cartridges were connected to the installed gas samplers. The soil atmosphere of the corresponding depth was then pumped with an airflow of 7 mL min^1 over a desiccant (Drierite, W. A. Hammond Drierite Company, USA) to the molecular sieve cartridge for 40 minutes to trap the CO_2 on the molecular sieve. Surface samples were taken from a respiration chamber (Gaudinsik et al., 2000). The atmospheric CO_2 inside the chamber was removed prior to sampling by circulating an airflow of $\approx$ 1.5 L min^{-1} from the chamber through a column filled with soda lime until the equivalent of 2-3 chamber volumes had been passed over the soda lime. Thereafter, the airflow was run over a desiccant and the molecular sieve cartridge for 10 minutes to collect the CO_2 sample.

In the laboratory, the adsorbed CO_2 was released from the molecular sieve cartridge by heating the molecular sieve under vacuum (Wotte et al., 2017). The released CO_2 was purified cryogenically and sealed in a glass tube. The radiocarbon (^{14}C) analysis was directly performed on the CO_2 with the gas ion source of the mini carbon dating system (MICADAS, Ionplus, Switzerland) at ETH Zurich (Ruff et al., 2010). The ^{14}C concentrations are reported as fraction modern carbon ($F^{14}C$), whereby $F^{14}C$ values less than one denote that the majority of the C was fixed before the nuclear bomb tests in the 1960s, while values greater than one indicate C fixation after the bomb tests.

2.3 Labelling experiment

To trace the fate of fresh litter inputs in the soil and their contribution to the CO_2 released from different soil horizons, a ^{13}C labelling experiment was performed. In January 2015, the leaf litter layer around the subsoil observatories was removed and replaced with a homogeneous mixture of 237 g ^{13}C-labelled and 1575 g non-labelled young beech litter, which is equal to a litter input of 250 g m^{-2}. The labelled litter was distributed on a semi-circular area around the subsoil observatories. The labelled litter originated from young beech trees grown in a greenhouse in a $^{13}CO_2$-enriched atmosphere. The mixture of labelled and non-labelled litter had an average $\delta^{13}C$ value of 1241 ‰ for subsoil observatory 1 (OB1) and a $\delta^{13}C$ value of 1880 ‰ for subsoil observatories 2 (OB2) and 3 (OB3).

2.4 Diffusivity measurements

Gas transport along the soil profile is determined by the diffusivity of the soil. The diffusivity of the soil was determined at depths of 10, 30, 50, 90 and 150 cm, with five undisturbed core sample replicates per depth and per observatory. To account for different water contents, the undisturbed soil cores (5.7 cm diameter, 4.0 cm height) were adjusted in the laboratory at different matrix potentials (-30 hPa, -60 hPa, -300 hPa) to cover a wide range of soil moisture. After moisture adjustment, the soil cores were attached to a diffusion chamber as described in Böttcher et al. (2011). The diffusion chamber was flushed with N_2 to initially establish a gas gradient between the chamber and the top of the sample as an atmospheric boundary condition. The increase in oxygen inside the ventilated chamber was measured over time with an oxygen dipping probe (DP-PSt3-L2.5-St10-YOP, PreSens-Precision Sensing GmbH, Germany). Diffusivity and tortuosity factors (τ) were calculated with an inverse diffusion model (Schwen and Böttcher, 2013).

Biogeosciences Discuss., https://doi.org/10.5194/bg-2019-143
Manuscript under review for journal Biogeosciences
Discussion started: 26 April 2019

2.5 Data analysis

2.5.1 Gradient method

This method is based on the assumption that molecular diffusion is the main gas transport in the soil atmosphere. Therefore gas fluxes, e.g. CO_2 fluxes in a soil profile, can be calculated from the CO_2 concentration gradient and the effective gas diffusion coefficient in the specific soil layer of interest.

In order to account for temperature and pressure dependencies of the CO_2 sensors, the CO_2 concentrations were corrected with a compensation algorithm for the GMP221 (S1) provided by the manufacturer (pers. comm. Niklas Piiroinen, Vaisala Oyi, Finland). For the flux calculation, CO_2 volume concentrations were converted to CO_2 mole concentrations (2):

$$C = \frac{C_v \times p}{R \times T} \tag{2}$$

where C is the CO_2 mole concentration [µmol m^{-3}], C_v is the CO_2 volume fraction [µmol mol^{-1}], p is the atmospheric pressure in [Pa], R is the universal gas constant [8.3144 J K^{-1} mol^{-1}] and T is the soil temperature in [K] measured by temperature sensors at the corresponding soil depths. The CO_2 flux of a soil layer was calculated using Fick's first law (Eq. 3)

$$F = -D_s \times \frac{dC}{dz} \tag{3}$$

where F is the diffusive CO_2 flux [µmol m^{-2} s^{-1}], D_s is the effective diffusivity in the soil atmosphere [m^2 s^{-1}] determined as described below, C is the CO_2 concentration [µmol m^{-3}] and z is the depth [m]. The equation is based on the assumption that 1) molecular diffusion is the dominating transport process in the soil atmosphere and other transport mechanisms – i.e. convective CO_2 transport due to air pressure gradients or diffusion in the soil, and convective transport with soil water – are negligible and 2) gas transport is one-dimensional (e.g., de Jong, E., Schappert, 1972; Maier and Schack-Kirchner, 2014). The effective diffusivity D_s was calculated with Eq. 4:

$$D_s = D_0 \times \tau \tag{4}$$

where D_0 is the CO_2 diffusivity in free air. The pressure and temperature effect on D_0 were taken into account by:

$$D_0 = D_{a0} \times \left(\frac{p_0}{p}\right) \times \left(\frac{T}{T_0}\right)^{1.75} \tag{5}$$

where D_{a0} is a reference value of D_0 at standard conditions (1.47×10^{-5} m^2 s^{-1} at T_0 293.15 K and p_0 1.013×10^5 Pa) (Jones, 1994). The dimensionless tortuosity factor τ at each depth was modelled as a function of the air-filled pore space ε for each soil depth. The model was derived from a power function fit from laboratory diffusion experiments (see above) on the undisturbed soil cores.

To account for the non-uniform vertical distribution of soil water content in the soil profile, D_s was estimated as the harmonic average between the two measurement depths (Pingintha et al., 2010; Turcu et al., 2005):

$$D_s = \frac{\Delta z_1 + \Delta z_2}{\frac{\Delta z_1}{D_{s z_1}} + \frac{\Delta z_2}{D_{s z_2}}} \tag{6}$$

Biogeosciences Discuss., https://doi.org/10.5194/bg-2019-143
Manuscript under review for journal Biogeosciences
Discussion started: 26 April 2019

where $\Delta z_{1,2}$ [m] is the thickness of the corresponding soil layer and $D_{sz_{1,2}}$ is the effective diffusivity of the respective soil layer. Finally, assuming a constant flux between measured CO_2 at depth z_i and z_{i+1}, the CO_2 flux (F_i) was calculated by combining Eq. (2 - 6)

$$F_i = \left(\frac{\Delta z_i + \Delta z_{i+1}}{\frac{\Delta z_i}{D_{sz_i}} + \frac{\Delta z_{i+1}}{D_{sz_{i+1}}}} \right) \times \left(\frac{C_{i+1} - C_i}{z_{i+1} - z_i} \right) \quad (7)$$

where F_i is the CO_2 flux [µmol m^{-2} s^{-1}] at the upper boundary (z_i) between depth z_i and z_{i+1}[m]. To calculate soil respiration (F_0) at the surface with the gradient method, a CO_2 concentration of 400 µmol mol^{-1} at the soil surface and a constant D_s for the first 10 cm were assumed.

2.5.2 CO_2 production

The CO_2 production (P_i) in a soil layer was calculated as the difference between the flux (F_i) leaving the specific soil layer at the upper boundary (z_i) and the input flux (F_{i+1}) at the lower boundary (z_{i+1}) of the specific soil layer. Therefore, P_i had the unit of a flux [µmol m^{-2} s^{-1}].

$$P_i = F_i - F_{i+1} \quad (8)$$

Total soil respiration was calculated as the sum of CO_2 production in all soil layers. Equation (8) is based on the assumption of steady-state diffusion. Steady-state conditions for CO_2 concentration and volumetric water content were mostly given, except during a few heavy rain events where steady-state conditions were not met due to changing water contents in the profiles. Most soils exhibit increasing CO_2 concentrations with increasing soil depth. Therefore, CO_2 production is mostly positive with upward CO_2 fluxes. However, if the CO_2 concentration in a soil layer is greater than in the layers below, the calculated CO_2 production in the layers below can become negative (downward directed). Hence in the present study no CO_2 production was assumed when the calculated CO_2 production in a soil layer was negative. This approach was based on the assumption that there are no relevant CO_2 sinks in the soil profile. Furthermore, negative CO_2 production is considered as CO_2 storage, which will be released if the CO_2 concentration gradient or diffusion conditions change. In OB1 negative CO_2 production values were calculated in the first year at 30-50 cm depth (331 out of 365) and at 50-90 cm depth (359 out of 365). In the second year negative values also occurred in OB1 at 30-50 cm depth (8 out of 308) and at 50-90 cm depth (182 out of 308).

2.5.3 Isotopic composition of CO_2

To determine the contribution of labelled leaf litter to CO_2 in different soil layers, the fluxes of $^{12}CO_2$ and $^{13}CO_2$ had to be calculated separately. Therefore, the amount of $^{13}CO_2$ (L) originating from the labelled leaf litter was calculated using the isotopic mixing equation (Eq. 9):

$$L = 1 - \left(\frac{\delta^{13}C_M - \delta^{13}C_L}{\delta^{13}C_B - \delta^{13}C_L} \right) \quad (9)$$

where $\delta^{13}C_M$ is the isotopic signature of the gas sample, $\delta^{13}C_L$ is the isotopic signature of the labelled leaf litter and $\delta^{13}C_B$ is the average isotopic signature of the gas samples before the labelled leaf litter was applied. The $^{13}CO_2$ volume concentration

Biogeosciences Discuss., https://doi.org/10.5194/bg-2019-143
Manuscript under review for journal Biogeosciences
Discussion started: 26 April 2019

for each layer was calculated using Eq. (2) multiplied by *L*. The $^{13}CO_2$ fluxes and production rates were calculated using Eq. (3)-(8). To account for different effective diffusivities of $^{12}CO_2$ and $^{13}CO_2$, the effective diffusivity D_s for $^{13}CO_2$ was adjusted according to Cerling et al. (1991):

$$D_s = {}^{12}D_s = 1.0044 \times {}^{13}D_s \tag{10}$$

where it is assumed that D_s is equivalent to ${}^{12}D_s$ due to the fact that about 99 % of total CO_2 is $^{12}CO_2$.

2.6 Statistical analysis

A Monte Carlo simulation was generated to determine the influence of measurement uncertainties of the sensors, which were used for calculation of CO_2 fluxes and CO_2 production rates . It was assumed that each measurement error was normally distributed. The standard deviation was equal to measurement accuracy, which was obtained from the corresponding manual. To obtain a distribution of the power function (D_s model), the Markov chain Monte Carlo algorithm DiffeRential Evolution Adaptive Metropolis (DREAM) (Vrugt et al., 2009) in the R package dream (Guillaume and Andrews, 2012) was used. Dream was run in the standard configuration and as soon as the convergence criteria of Gelman and Rubin (1992)were less than 1.01, another 20000 simulations were run to get a distribution of the D_s model parameters (n=1000). The distributions of CO_2, volumetric water content and temperature measurements and the distribution of the *Ds* model were used for 1000 Monte Carlo simulations. Unless stated otherwise, the error bars in the final results represent the standard deviation of these simulations. All analyses were performed in R (version 3.3.2) for Linux (R Core Team, 2017).

3 Results

3.1 Temperature, water content and CO_2 concentration in the profile

Soil temperature showed a distinct seasonality down to 150 cm, with the maximum and the minimum temperatures delayed with increasing soil depth (Fig. 1a). The minimum soil temperature was 0.3 °C and 4.0 °C in January 2016 at 10 cm and 150 cm depths respectively. The maximum temperature was measured in July in the uppermost layer (16.6 °C) and in August in the deepest layer (14.4 °C). The annual amplitude of soil temperature decreased from 16.3 °C at 10 cm to 10.4 °C at 150 cm. However, mean annual values showed no significant decline with soil depth and were 8.4 °C and 8.3 °C at 10 cm and 150 cm respectively during the two years of observation. Variations in the mean soil temperatures between the three observatories were < 1 °C at all depths (Fig. S1).

The volumetric water contents also showed seasonal variations at all depths (Fig. 1b), with depletion during the summer. The minimum of volumetric water content at 10 cm was reached in August (10 %), whereas the minimum at 150 cm was observed two months later in October (6 %). The water reservoir of the soil profile was refilled during the autumn and winter, reaching maximum values at 10 cm (23 %) and 150 cm (22 %) in April (Fig. 1b), which were delayed by 14 days in the deepest layer. In OB1 and OB3, the mean volumetric water content decreased with increasing soil depth. Only in OB2 did the mean water

content increase at 150 cm (Fig. S2). The water content showed a greater variation between the three observatories than soil temperature (Fig. S2).

The CO_2 concentration in the soil pores followed a similar seasonality as soil temperature (Fig. 1c), with a maximum during the summer and a minimum during the winter and early spring. The same behaviour was observed for both investigated years, while the values were higher during the first summer. The CO_2 concentration in the uppermost layer ranged from 1,000 to 35,000 µmol mol^{-1} and thus was in a similar range of results for the deepest layer with 7,500 to 35,000 µmol mol^{-1}. However, values were highly variable between the observatories, with OB2 and OB3 showing an increasing CO_2 concentration with greater soil depth, whereas OB1 yielded the highest CO_2 concentrations at 30 to 50 cm depth.

3.2 Soil respiration

The mean annual mineral (without the organic layer) soil respiration determined with chamber measurements for the three observatories was 776 ± 193 g C m^{-2} yr^{-1}, with a small variability between the observatories (Table 1). The mineral soil respiration modelled with the Lloyd-Taylor function gave similar results for the same period. In contrast, soil respiration determined with the gradient method showed a high variability between the observatories, but was in the range of the directly measured respiration, except for OB1. This variability can be explained by the higher water content at OB1 and consequently the lower diffusion coefficient. The average diffusion coefficient at OB1 at 10 cm was less than half that at OB2 and OB3.

The organic layer increased total respiration by 13 % and 25 % respectively for the Lloyd-Taylor model and chamber measurements (Table 1). For all the methods and in all the observatories, soil respiration correlated well with soil temperature and soil moisture. The highest fluxes were measured when soil temperature (10 cm) was highest and water content (10 cm) was low (Fig. 1 and Fig. 2).

3.3 Vertical CO_2 production

The mean CO_2 production rates decreased from 1.4 µmol m^{-2} s^{-1} in the uppermost layer (0–10 cm depth) to 0.03 µmol m^{-2} s^{-1} in the deepest layer (50–90 cm depth) (Fig. 3). The CO_2 production followed the same seasonality as soil temperature and CO_2 concentration, with the highest productions rates occurring during the summer and the lowest during the winter months in all soil layers. This seasonal variation was greatest in the top two layers of the soil (0–10, 10–30 cm) (Fig. 3a-d).

About 71 ± 10 % of total soil respiration was produced in the first 10 cm of the soil profile where 21 % of the SOC stock (0–1.5 m) was stored. The CO_2 production at 10 to 30 cm accounted for 18 ± 11 % of total soil respiration during the year, and 32 % of the SOC was located in this depth increment. The subsoil (> 30 cm) accounted for 10 ± 8 % of total CO_2 production, with 47 % of the SOC stock stored in the subsoil.

The mean total CO_2 production showed no significant differences between the two years. The variation in cumulative annual CO_2 production was greater between the three observatories (335–1,203 g CO_2-C m^{-2} yr^{-1}) than between the two studied years (Fig. 4). However, the CO_2 production in the different soil layers showed considerable changes with time: it increased by 500 % in the subsoil from 30 to 50 cm in the second year, which increased the contribution of subsoil CO_2 production from 3 % to 15 % of total CO_2 production. This increase was observed in all three observatories. In contrast, the CO_2 production in the

first 10 cm in OB1 and OB3 showed a decline from the first to the second year, which was probably caused by methodological variations and does not represent a real decrease in respiration activity since bioturbation of animals (e.g. voles) might have had a strong influence on diffusivity (Fig. 3a). Voles created macropores, therefore the CO_2 gradient approach was not applicable. This was also indicated by a sudden and rapid drop of CO_2 production between 0 and 10 cm in OB1 (October 2015) (Fig. 3a).

To take the different SOC contents of each soil layer into account, the cumulative CO_2 production was normalised to the SOC stock of the respective layer (Fig. 5). The specific CO_2 production decreased from 346 g CO_2-C kg^{-1} SOC yr^{-1} in the first 10 cm to less than 8 g CO_2-C kg^{-1} SOC yr^{-1} at 50 to 90 cm. It should be noted that the proportion of autotrophic respiration in the total CO_2 production could not be quantified.

3.4 Sources of CO_2 production

3.4.1 Contribution of fresh litter

The isotopic signature of soil CO_2 ($\delta^{13}CO_2$) in the observatories before the start of labelling experiment ranged from -25.4 ‰ to -21.8 ‰, with no significant differences between soil depths (Fig. 6a). The labelling experiment was conducted to assess the fate of fresh litter added on top of the organic layer into different C fractions (e.g. SOC and DOC) including soil CO_2. Six days after the application of the ^{13}C-labelled leaf litter, CO_2 was already enriched in litter-derived C down to 90 cm depth in all the observatories. The isotopic signature ranged from 70 ‰ at 10 cm depth to -19 ‰ at 90 cm depth (Fig. 6b). Thus, the maximum contribution of litter-derived C to total CO_2 was 5 % at 10 cm depth six days after the litter replacement (Fig. 6c). At 90 cm, the maximum amount of litter-derived CO_2 was 0.6 % two weeks after the beginning of the labelling experiment (Fig. 6c). In addition, minor peaks with up to 0.8 % of CO_2 derived from the labelled litter were observed at all depths after rain events within the first six months of litter application. However, the average contribution of litter-derived CO_2 decreased with time and reached a range of 2.5 % to 0.2 % at 10 cm depth from January 2015 to July 2016.

Assuming that diffusion is the main transport process of CO_2 in the soil atmosphere, the litter-derived CO_2 flux between two soil layers can be calculated according to Eq. (3-7) and Eq. (10). As already mentioned, a positive flux indicates mineralisation of litter-derived C in the respective soil layer. A negative flux in turn represents downward diffusion of litter-derived CO_2 from the layer above (Fig. 7). On average for the three observatories, 34 out of 41 sampling days had negative $^{13}CO_2$ fluxes, indicating a downward movement of labelled litter-derived CO_2. Only OB1 had positive $^{13}CO_2$ fluxes at 10 to 50 cm, representing a transport of labelled litter-derived C down the soil profile as dissolved organic carbon (DOC) and mineralisation of this DOC. The observed ^{13}C enrichment in CO_2 in OB2 and OB3 was due to diffusion of labelled litter-derived CO_2 from the organic layer down to deeper layers of the mineral soil.

3.4.2 Contribution of old C

The radiocarbon content of the bulk SOC decreased strongly with increasing soil depth from close to atmospheric values ($F^{14}C$ 0.99) at 10 cm to an apparent age of about 3460 years BP ($F^{14}C$ 0.65) at 110 cm depth (Fig. 9, grey triangles). In contrast, the ^{14}C concentrations of the CO_2 in the soil atmosphere were relatively constant throughout the soil profile and for

both samplings, with values in the range of 1.03–1.07 $F^{14}C$ and thus derive mainly from the post-bomb period (Fig. 8, black dots). This indicates a young source of CO_2 production. Consequently "old" subsoil SOC was not detected as a significant source of CO_2 production.

4 Discussion

4.1 Temperature, water content and CO_2 concentration in the profile

In all three subsoil observatories, increasing CO_2 concentrations with depth were observed. This has also been reported by other studies (Davidson et al., 2006; Drewitt et al., 2005; Fierer et al., 2005; Hashimoto et al., 2007; Moyes and Bowling, 2012). However, the increase was not continuous down to 150 cm depth. Higher CO_2 concentrations were observed between 30 cm and 50 cm depth, indicating a higher CO_2 production at this depth increment, which can be linked to the root distribution in the subsoil observatories (9). About 82 % of the fine root biomass and necromass were found to be located between 0 and 50 cm, and 18 % at the 30 to 50 cm depth. Therefore, the contribution of autotrophic respiration to CO_2 production and the mineralisation of dead roots were greater at these depths than in the deep subsoil (> 50 cm). The CO_2 concentration in the soil pores is also controlled by abiotic factors such as effective diffusivity (D_s). The average effective diffusivity (D_s) at 10 cm was about 40 % lower than at 30 cm. Consequently CO_2 accumulated in the soil pores below 10 cm depth due to the lower diffusion of CO_2 between the soil surface and 10 cm depth. The effective diffusivity was mainly controlled by soil water content, which reduced it. For example, the high CO_2 concentration in August 2014 (up to 40,000 µmol mol^{-1}) compared to August 2015 (up to 20,000 µmol mol^{-1}) (1c) can be explained by the higher volumetric water content in 2014 in all profiles. The high water content was related to more precipitation in July 2014 (120 mm) than in July 2015 (47 mm) and to less precipitation in August in both years (49 and 95 mm). Additionally, evapotranspiration was greater in August 2015 than in August 2014 due to a higher mean air temperature (18 °C and 15 °C).

4.2 Soil respiration

The annual mean total respiration determined using the gradient method corresponded well with the results of the closed chamber measurements, indicating that the gradient method resulted in realistic flux estimations (Table 1, Fig. 2). This is in line with the results reported by other studies (Baldocchi et al., 2006; Tang et al., 2003; Liang et al., 2004). The differences in soil respiration between the methods can be attributed to the different spatial resolution of the corresponding measurements. The chamber measurements were based on five spatial replicates for each subsoil observatory, covering a total measurement area of 1274 cm^2. Therefore chamber measurements accounted for spatial variability in water content and soil CO_2 concentrations below the chamber, whereas the gradient method was based on one profile measurement for CO_2 and water content at each of the three observatories. Large differences in total respiration rates of up to 200 % were found between the three observatories with the gradient method. Both methods have advantages and disadvantages for determining total soil respiration. The gradient method does not alter the soil atmosphere CO_2 gradient and is continuous and less time-consuming than chamber measure-

ments, but it is very vulnerable to the spatial heterogeneity of the soil structure and moisture content around the sensors and to changes in diffusivity, e.g. due to bioturbation by animals such as voles, which may also led to an underestimation of total soil respiration (e.g. OB1 Fig. 3a).

4.3 Vertical CO_2 production

The vertically partitioned CO_2 flux revealed that more than 90 % of total CO_2 efflux was produced in the topsoil (< 30 cm). These results correspond well with other studies which have found that more than 70 % of total CO_2 efflux in temperate forests is produced in the upper 30 cm of the soil profile (Davidson et al., 2006; Fierer et al., 2005; Hashimoto et al., 2007; Jassal et al., 2005; Moyes and Bowling, 2012). However, only 53 % of the SOC stock is stored in the first 30 cm, indicating that subsoil SOC on the site of the present study may have a slower turnover than topsoil SOC. This is supported by the low ^{14}C concentrations in SOC below 30 cm. However, the higher CO_2 production in the topsoil can be also related to greater fine root biomass and necromass density (Fig. 9, which may serve as an indicator of autotrophic respiration and heterotrophic respiration in the rhizosphere. Consequently root-derived respiration is greater in the topsoil than in the subsoil.

It is remarkable that the CO_2 production at 30 to 50 cm increased from 23 g C m^{-2} yr^{-1} in the first year to 118 g C m^{-2} yr^{-1} in the second year of the study (Fig. 4). This can be explained in part by more precipitation in the second year (621 mm) than in the first year (409 mm), inducing less water-limiting conditions for plants and microbial activity. As a result, the mean volumetric water content was higher in the second year (18 % compared to 16 %) at 50 cm depth, which gave better conditions for the mineralisation of SOC by microorganisms (Cook et al., 1985; Moyano et al., 2012). Furthermore, the greater precipitation increased the input of DOC into the subsoil on the site of the present study, which is supported by the study of (Leinemann et al., 2016) who investigated DOC fluxes in subsoil observatories for more than 60 weeks. They found a positive correlation between DOC fluxes, precipitation and water fluxes at 10, 50 and 150 cm depths. Furthermore, they showed that DOC fluxes declined by 92 % between a depth of 10 cm and 50 cm, which was attributed to mineral adsorption and microbial respiration of DOC (Leinemann et al., 2016).

4.4 Sources of CO_2 production

4.4.1 Young litter derived CO_2

In this study, a unique labelling approach was used to estimate the contribution of aboveground litter to CO_2 production along a soil profile by applying stable isotope-enriched leaf litter to the soil surface. These results showed that litter-derived C did not significantly contribute to annual CO_2 production below 10 cm depth. Leaf litter is decomposed and washed into the mineral soil as DOC. Within one year, only 0.2 % of total CO_2 production between 10 and 50 cm originated from the labelled leaf litter. Below 50 cm there was no contribution of litter-derived C to CO_2 production. Therefore, mineralisation of DOC originating from the organic layer was a minor source of CO_2 production in the soil profile below 10 cm. The average DOC flux in the subsoil observatories in the first year was estimated to be 20 g C m^{-2} yr^{-1} at 10 cm depth and 2 g C m^{-2} yr^{-1} at 50 cm depth, indicating a DOC input of 18 g C m^{-2} yr^{-1} into the 10 and 50 cm depth increments (Leinemann et al., 2016). An assumed

complete mineralisation of this DOC would account for 11 % of CO_2 production at this depth increment. Overall, most of the CO_2 production between a depth of 10 cm and 50 cm must be derived from autotrophic respiration and heterotrophic respiration in the rhizosphere.

4.4.2 Old SOC derived CO_2

The very similar radiocarbon contents of soil CO_2 produced at different depths, which were 1.06 $F^{14}C$ on average, revealed that ancient SOC components were not a major source of CO_2 production. The results indicate that the CO_2 originated mainly from young (several decades old) C sources, presumably mainly from root respiration, its exudates and DOC. Other studies have found similar results on a grassland site in California down to 230 cm depth (Fierer et al., 2005) and in temperate forests down to 100 cm (Gaudinsik et al., 2000; Hicks Pries et al., 2017). In addition, Hicks Pries et al. (2017) incubated root-free soil from three depths (15, 50 and 90 cm) and compared the radiocarbon signature of the respired CO_2 with their results from the field. They found that CO_2 from the short-term incubations had the same modern signature as the field measurements, despite the high ^{14}C age of the bulk SOC at 90 cm depth (˜1000 yr BP) (Hicks Pries et al., 2017). This supports the findings of the present experiment. Therefore, microbial respiration in temperate subsoils is mainly fed by relatively young C sources fixed less than 60 years ago.

4.4.3 Diffusion effects

A highly ^{13}C-enriched CO_2 source was introduced to the top of a soil profile. Shortly afterwards the application an enrichment of ^{13}C was measured in CO_2 along the whole soil profile (Fig. 6b). However, this enrichment could not be linked to the transport and mineralisation of litter-derived C along the soil profile (e.g. DOC in seepage water). In contrast, diffusion of $^{13}CO_2$ was observed to have originated from the mineralisation in the litter layer down the soil profile. According to Fick's first law, $^{13}CO_2$ diffuses into the soil profile following the $^{13}CO_2$ gradient independently from the $^{12}CO_2$. Thus even though the total CO_2 concentration increased with soil depth, meaning an upward diffusion of $^{12}CO_2$, the $^{13}CO_2$ gradient was the opposite due to ^{13}C-enriched leaf litter leading to a downward diffusion of $^{13}CO_2$. Consequently this could lead to a misinterpretation of the pathways of subsoil $^{13}CO_2$ in tracer experiments. Furthermore, this effect should also be taken into consideration when interpreting $^{14}CO_2$ soil profile measurements as an indicator of the age of the mineralised SOC, as in other field studies (e.g., Davidson et al., 2006; Davidson and Trumbore, 1995; Fierer et al., 2005; Gaudinsik et al., 2000). Downward diffusion of $^{14}CO_2$ might be an important factor for explaining the observed $^{14}CO_2$ profiles. If this downward diffusion is the case, the $^{14}CO_2$ gradient should not have a continuous decrease with soil depth since the $^{14}CO_2$ gradient is the driving factor for diffusion according to Eq. (3). In fact, $^{14}CO_2$ concentration at 30 cm depth in subsoil OB1 was greater than at 50 cm depth (Fig. 10), which in turn led to a downward diffusion of $^{14}CO_2$ from a depth of 30 cm to 50 cm. This might lead to a rejuvenation of the $^{14}CO_2$ soil profile and to an underestimation of the mineralisation of old SOC in subsoils.

Biogeosciences Discuss., https://doi.org/10.5194/bg-2019-143
Manuscript under review for journal Biogeosciences
Discussion started: 26 April 2019

5 Conclusions

The gradient method allowed total soil respiration to be partitioned vertically along a soil profile. Most of the CO_2 (90 %) was produced in the topsoil (< 30 cm). However, the subsoil (> 30 cm), which contained 47 % of SOC stocks, accounted for 10 % of total soil respiration. This can be explained by a larger amount of stable SOC in subsoils as compared to topsoils. However, the modern radiocarbon signature of CO_2 throughout the soil profiles indicated that mainly young carbon sources were being respired, such as from roots and root exudates and autotrophic respiration. The contribution of old SOC to subsoil CO_2 production was too small to significantly alter the ^{14}C concentrations in the soil atmosphere used to identify CO_2 sources. Furthermore, this study showed that the mineralisation of fresh litter-derived C only contributed to a small part of total soil respiration, underlining the importance of roots and the rhizosphere for subsoil CO_2 production.

Author contributions. All the authors contributed to the design of the field measurements and PWD carried out the field measurements. Preparation of 14CO2 samples was performed by PWD and AW. Data analysis and modelling were performed by PWD. KK took the root samples and analysed them and provided the data. PWD took the lead in writing the manuscript, with contributions from all the co-authors.

Competing interests. The authors declare that they have no conflict of interest.

Acknowledgements. This study was funded by the Deutsche Forschungsgemeinschaft (DFG) (HE 6877/1-1) within the framework of the research unit SUBSOM (FOR1806) – "The Forgotten Part of Carbon Cycling: Organic Matter Storage and Turnover in Subsoils". We would like to thank Jens Dyckmanns and Reinhard Langel from the Centre for Stable Isotope Research and Analysis at the University of Göttingen for $^{13}13CO_2$ measurements. We also want to thank Frank Hegewald and Martin Volkmann for their support in the field, especially changing the 23 kg heavy batteries in the subsoil observatories every month. We would also like to thank Ullrich Dettmann for his support with R. Last but not least, many thanks to Marco Gronwald, Cora Vos and Viridiana Alcantara for fruitful discussions and recommendations.

References

Agnelli, A., Ascher, J., Corti, G., Ceccherini, M. T., Nannipieri, P., and Pietramellara, G.: Distribution of microbial communities in a forest soil profile investigated by microbial biomass, soil respiration and DGGE of total and extracellular DNA, Soil Biology and Biochemistry, 36, 859–868, https://doi.org/10.1016/j.soilbio.2004.02.004, http://www.sciencedirect.com/science/article/pii/S0038071704000549http://linkinghub.elsevier.com/retrieve/pii/S0038071704000549, 2004.

Angst, G., John, S., Mueller, C. W., Kögel-Knabner, I., and Rethemeyer, J.: Tracing the sources and spatial distribution of organic carbon in subsoils using a multi-biomarker approach, Scientific Reports, 6, 29 478, https://doi.org/10.1038/srep29478, http://www.nature.com/articles/srep29478, 2016.

Baldocchi, D., Tang, J., and Xu, L.: How switches and lags in biophysical regulators affect spatial-temporal variation of soil respiration in an oak-grass savanna, Journal of Geophysical Research: Biogeosciences, 111, n/a–n/a, https://doi.org/10.1029/2005JG000063, http://doi.wiley.com/10.1029/2005JG000063, 2006.

Batjes, N. H.: Total carbon and nitrogen in the soils of the world, European Journal of Soil Science, 65, 10–21, https://doi.org/10.1111/ejss.12114_2, http://doi.wiley.com/10.1111/ejss.12114{_}2, 2014.

Bond-Lamberty, B. and Thomson, A.: Temperature-associated increases in the global soil respiration record, Nature, 464, 579–582, https://doi.org/10.1038/nature08930, http://www.nature.com/doifinder/10.1038/nature08930, 2010.

Bond-Lamberty, B., Bailey, V. L., Chen, M., Gough, C. M., and Vargas, R.: Globally rising soil heterotrophic respiration over recent decades, Nature, 560, 80–83, https://doi.org/10.1038/s41586-018-0358-x, http://www.nature.com/articles/s41586-018-0358-x, 2018.

Borken, W., Xu, Y.-J., Davidson, E. A., and Beese, F.: Site and temporal variation of soil respiration in European beech, Norway spruce, and Scots pine forests, Global Change Biology, 8, 1205–1216, https://doi.org/10.1046/j.1365-2486.2002.00547.x, http://doi.wiley.com/10.1046/j.1365-2486.2002.00547.x, 2002.

Böttcher, J., Weymann, D., Well, R., Von Der Heide, C., Schwen, A., Flessa, H., and Duijnisveld, W. H. M.: Emission of groundwater-derived nitrous oxide into the atmosphere: Model simulations based on a 15N field experiment, European Journal of Soil Science, 62, 216–225, https://doi.org/10.1111/j.1365-2389.2010.01311.x, 2011.

Cerling, T. E., Solomon, D., Quade, J., and Bowman, J. R.: On the isotopic composition of carbon in soil carbon dioxide, Geochimica et Cosmochimica Acta, 55, 3403–3405, https://doi.org/10.1016/0016-7037(91)90498-T, http://linkinghub.elsevier.com/retrieve/pii/001670379190498T, 1991.

Cook, F. J., Orchard, V. A., and Corderoy, D. M.: Effects of lime and water content on soil respiration, New Zealand Journal of Agricultural Research, 28, 517–523, https://doi.org/10.1080/00288233.1985.10417997, http://www.tandfonline.com/doi/full/10.1080/00288233.1985.10417997, 1985.

Davidson, E., Savage, K., Trumbore, S., and Borken, W.: Vertical partitioning of CO2 production within a temperate forest soil, Global Change Biology, 12, 944–956, https://doi.org/10.1111/j.1365-2486.2006.01142.x, 2006.

Davidson, E. a. and Trumbore, S. E.: Gas diffusivity and production of CO2 in deep soils of the eastern Amazon, Tellus B, 47, 550–565, https://doi.org/10.3402/tellusb.v47i5.16071, http://www.tellusb.net/index.php/tellusb/article/view/16071, 1995.

Davidson, E. A., Belk, E., and Boone, R. D.: Soil water content and temperature as independent or confounded factors controlling soil respiration in a temperate mixed hardwood forest, Global Change Biology, 4, 217–227, https://doi.org/10.1046/j.1365-2486.1998.00128.x, http://doi.wiley.com/10.1046/j.1365-2486.1998.00128.x, 1998.

de Jong, E., Schappert, H.: Calculation of soil respiration and activity from CO2 profiles in the soil, Soil Science, 113, 328–333, http://journals.lww.com/soilsci/Fulltext/1972/05000/CALCULATION{_}OF{_}SOIL{_}RESPIRATION{_}AND{_}ACTIVITY{_}FROM.6.aspxhttp://www.ncbi.nlm.nih.gov/pubmed/731, 1972.

Drewitt, G. B., Black, T. A., and Jassal, R. S.: Using measurements of soil CO2 efflux and concentrations to infer the depth distribution of CO2 production in a forest soil, Canadian Journal of Soil Science, 85, 213–221, https://doi.org/10.4141/S04-041, http://pubs.aic.ca/doi/abs/10.4141/S04-041http://www.nrcresearchpress.com/doi/10.4141/S04-041, 2005.

Fang, C. and Moncrieff, J.: The dependence of soil CO2 efflux on temperature, Soil Biology and Biochemistry, 33, 155–165, https://doi.org/10.1016/S0038-0717(00)00125-5, http://linkinghub.elsevier.com/retrieve/pii/S0038071700001255, 2001.

Fierer, N., Chadwick, O. A., and Trumbore, S. E.: Production of CO2 in soil profiles of a California annual grassland, Ecosystems, 8, 412–429, https://doi.org/10.1007/s10021-003-0151-y, http://link.springer.com/10.1007/s10021-003-0151-y, 2005.

Gaudinsik, J., Trumbore, S., Davidson, E., and Zheng, S.: Soil carbon cycling in a temperate forest: radiocarbon-based estimates of residence times, sequestration rates and partitioning of fluxes, Biogeochemistry, 51, 33–69, http://www.springerlink.com/content/u8488532841u73t7/, 2000.

Gelman, A. and Rubin, D. B.: Inference from Iterative Simulation Using Multiple Sequences, Statistical Science, 7, 457–472, https://doi.org/10.1214/ss/1177011136, http://projecteuclid.org/euclid.ss/1177011136, 1992.

Goffin, S., Aubinet, M., Maier, M., Plain, C., Schack-Kirchner, H., and Longdoz, B.: Characterization of the soil CO2 production and its carbon isotope composition in forest soil layers using the flux-gradient approach, Agricultural and Forest Meteorology, 188, 45–57, https://doi.org/10.1016/j.agrformet.2013.11.005, http://linkinghub.elsevier.com/retrieve/pii/S0168192313002955, 2014.

Guillaume, J. and Andrews, F.: dream: DiffeRential Evolution Adaptive Metropolis, https://r-forge.r-project.org/R/?group{_}id=545, 2012.

Hashimoto, S., Tanaka, N., Kume, T., Yoshifuji, N., Hotta, N., Tanaka, K., and Suzuki, M.: Seasonality of vertically partitioned soil CO2 production in temperate and tropical forest, Journal of Forest Research, 12, 209–221, https://doi.org/10.1007/s10310-007-0009-9, http://link.springer.com/10.1007/s10310-007-0009-9, 2007.

Hashimoto, S., Carvalhais, N., Ito, A., Migliavacca, M., Nishina, K., and Reichstein, M.: Global spatiotemporal distribution of soil respiration modeled using a global database, Biogeosciences, 12, 4121–4132, https://doi.org/10.5194/bg-12-4121-2015, https://www.biogeosciences.net/12/4121/2015/, 2015.

Heinze, S., Ludwig, B., Piepho, H.-p., Mikutta, R., Don, A., Wordell-Dietrich, P., Helfrich, M., Hertel, D., Leuschner, C., Kirfel, K., Kandeler, E., Preusser, S., Guggenberger, G., Leinemann, T., and Marschner, B.: Factors controlling the variability of organic matter in the top- and subsoil of a sandy Dystric Cambisol under beech forest, Geoderma, 311, 37–44, https://doi.org/10.1016/j.geoderma.2017.09.028, http://linkinghub.elsevier.com/retrieve/pii/S001670611731279Xhttp://dx.doi.org/10.1016/j.geoderma.2017.09.028https://linkinghub.elsevier.com/retrieve/pii/S001670611731279X, 2018.

Hicks Pries, C. E., Castanha, C., Porras, R. C., and Torn, M. S.: The whole-soil carbon flux in response to warming, Science, 355, 1420–1423, https://doi.org/10.1126/science.aal1319, http://science.sciencemag.org/content/355/6332/1420.fullhttp://www.sciencemag.org/lookup/doi/10.1126/science.aal1319, 2017.

Jassal, R., Black, A., Novak, M., Morgenstern, K., Nesic, Z., and Gaumont-Guay, D.: Relationship between soil CO2 concentrations and forest-floor CO2 effluxes, Agricultural and Forest Meteorology, 130, 176–192, https://doi.org/10.1016/j.agrformet.2005.03.005, http://dx.doi.org/10.1016/j.agrformet.2005.03.005, 2005.

Jobbágy, E. and Jackson, R.: The vertical distribution of soil organic carbon and its relation to climate and vegetation, Ecological applications, 10, 423–436, http://www.esajournals.org/doi/pdf/10.1890/1051-0761(2000)010[0423:TVDOSO]2.0.CO;2, 2000.

Jones, H. G.: Plants and microclimate :a quantitative approach to environmental plant physiology /, Cambridge Univ. Pr.,, Cambridge :, 2. ed., re edn., http://slubdd.de/katalog?TN{_}libero{_}mab2669667, 1994.

Leinemann, T., Mikutta, R., Kalbitz, K., Schaarschmidt, F., and Guggenberger, G.: Small scale variability of vertical water and dissolved organic matter fluxes in sandy Cambisol subsoils as revealed by segmented suction plates, Biogeochemistry, pp. 1–15, https://doi.org/10.1007/s10533-016-0259-8, http://link.springer.com/10.1007/s10533-016-0259-8, 2016.

Liang, N., Nakadai, T., Hirano, T., Qu, L., Koike, T., Fujinuma, Y., and Inoue, G.: In situ comparison of four approaches to estimating soil CO2 efflux in a northern larch (Larix kaempferi Sarg.) forest, Agricultural and Forest Meteorology, 123, 97–117, https://doi.org/10.1016/j.agrformet.2003.10.002, http://linkinghub.elsevier.com/retrieve/pii/S016819230300251Xhttp://dx.doi.org/10.1016/j.agrformet.2003.10.002, 2004.

Lloyd, J. and Taylor, J. A.: On the Temperature Dependence of Soil Respiration, Functional Ecology, 8, 315, https://doi.org/10.2307/2389824, http://www.jstor.org/stable/2389824?origin=crossref, 1994.

Maier, M. and Schack-Kirchner, H.: Using the gradient method to determine soil gas flux: A review, Agricultural and Forest Meteorology, 192-193, 78–95, https://doi.org/10.1016/j.agrformet.2014.03.006, http://dx.doi.org/10.1016/j.agrformet.2014.03.006http://linkinghub.elsevier.com/retrieve/pii/S0168192314000665, 2014.

Moyano, F. E., Vasilyeva, N., Bouckaert, L., Cook, F., Craine, J., Curiel Yuste, J., Don, A., Epron, D., Formanek, P., Franzluebbers, A., Ilstedt, U., Kätterer, T., Orchard, V., Reichstein, M., Rey, A., Ruamps, L., Subke, J. A., Thomsen, I. K., and Chenu, C.: The moisture response of soil heterotrophic respiration: Interaction with soil properties, Biogeosciences, 9, 1173–1182, https://doi.org/10.5194/bg-9-1173-2012, http://www.biogeosciences.net/9/1173/2012/, 2012.

Moyes, A. B. and Bowling, D. R.: Interannual variation in seasonal drivers of soil respiration in a semi-arid Rocky Mountain meadow, Biogeochemistry, 113, 683–697, https://doi.org/10.1007/s10533-012-9797-x, http://link.springer.com/article/10.1007/s10533-012-9797-x/fulltext.html, 2012.

Pingintha, N., Leclerc, M. Y., BEASLEY Jr., J. P., Zhang, G., and Senthong, C.: Assessment of the soil CO2 gradient method for soil CO2 efflux measurements: comparison of six models in the calculation of the relative gas diffusion coefficient, Tellus B, 62, 47–58, https://doi.org/10.1111/j.1600-0889.2009.00445.x, http://www.tellusb.net/index.php/tellusb/article/view/16512, 2010.

R Core Team: R: A Language and Environment for Statistical Computing, https://www.r-project.org/, 2017.

Raich, J. W. and Potter, C. S.: Global patterns of carbon dioxide emissions from soils, Global Biogeochemical Cycles, 9, 23–36, https://doi.org/10.1029/94GB02723, http://doi.wiley.com/10.1029/94GB02723, 1995.

Rethemeyer, J., Kramer, C., Gleixner, G., John, B., Yamashita, T., Flessa, H., Andersen, N., Nadeau, M. J., and Grootes, P. M.: Transformation of organic matter in agricultural soils: Radiocarbon concentration versus soil depth, Geoderma, 128, 94–105, https://doi.org/10.1016/j.geoderma.2004.12.017, http://www.sciencedirect.com/science/article/pii/S0016706104003283, 2005.

Ruff, M., Szidat, S., Gäggeler, H., Suter, M., Synal, H.-A., and Wacker, L.: Gaseous radiocarbon measurements of small samples, Nuclear Instruments and Methods in Physics Research Section B: Beam Interactions with Materials and Atoms, 268, 790–794, https://doi.org/10.1016/j.nimb.2009.10.032, http://dx.doi.org/10.1016/j.nimb.2009.10.032http://linkinghub.elsevier.com/retrieve/pii/S0168583X09010817, 2010.

Salomé, C., Nunan, N., Pouteau, V., Lerch, T. Z., and Chenu, C.: Carbon dynamics in topsoil and in subsoil may be controlled by different regulatory mechanisms, Global Change Biology, 16, 416–426, https://doi.org/10.1111/j.1365-2486.2009.01884.x, http://doi.wiley.com/10.1111/j.1365-2486.2009.01884.x, 2010.

Schindlbacher, A., Zechmeister-Boltenstern, S., and Jandl, R.: Carbon losses due to soil warming: Do autotrophic and heterotrophic soil respiration respond equally?, Global Change Biology, 15, 901–913, https://doi.org/10.1111/j.1365-2486.2008.01757.x, http://www.scopus.com/inward/record.url?eid=2-s2.0-61549114422{&}partnerID=40{&}md5=284ca82434a8cb5b3fea745b411eb272{%}5Cnhttp://onlinelibrary.wiley.com/doi/10.1111/j.1365-2486.2008.01757.x/abstract, 2009.

Schwen, A. and Böttcher, J.: A Simple Tool for the Inverse Estimation of Soil Gas Diffusion Coefficients, Soil Science Society of America Journal, 77, 759, https://doi.org/10.2136/sssaj2012.0347n, https://dl.sciencesocieties.org/publications/sssaj/abstracts/76/1/61https://www.soils.org/publications/sssaj/abstracts/77/3/759, 2013.

Suseela, V. and Dukes, J. S.: The responses of soil and rhizosphere respiration to simulated climatic changes vary by season, Ecology, 94, 403–413, https://doi.org/10.1890/12-0150.1, http://doi.wiley.com/10.1890/12-0150.1, 2013.

Tang, J., Baldocchi, D. D., Qi, Y., and Xu, L.: Assessing soil CO2 efflux using continuous measurements of CO2 profiles in soils with small solid-state sensors, Agricultural and Forest Meteorology, 118, 207–220, https://doi.org/10.1016/S0168-1923(03)00112-6, http://linkinghub.elsevier.com/retrieve/pii/S0168192303001126, 2003.

Tang, J., Misson, L., Gershenson, A., Cheng, W., and Goldstein, A. H.: Continuous measurements of soil respiration with and without roots in a ponderosa pine plantation in the Sierra Nevada Mountains, Agricultural and Forest Meteorology, 132, 212–227, https://doi.org/10.1016/j.agrformet.2005.07.011, http://linkinghub.elsevier.com/retrieve/pii/S0168192305001553, 2005.

Torn, M. S., Trumbore, S. E., Chadwick, O. A., Vitousek, P. M., and Hendricks, D. M.: Mineral control ofsoil organic carbon storage and turnover, Nature, 389, 170–173, https://doi.org/10.1038/38260, http://dx.doi.org/10.1038/38260http://www.nature.com/doifinder/10.1038/38260, 1997.

Turcu, V. E., Jones, S. B., and Or, D.: Continuous soil carbon dioxide and oxygen measurements and estimation of gradient-based gaseous flux, Vadose Zone Journal, 4, 1161–1169, https://doi.org/10.2136/vzj2004.0164, 2005.

Vrugt, J. a., ter Braak, C., Diks, C., Robinson, B. a., Hyman, J. M., and Higdon, D.: Accelerating Markov Chain Monte Carlo Simulation by Differential Evolution with Self-Adaptive Randomized Subspace Sampling, International Journal of Nonlinear Sciences and Numerical Simulation, 10, 273–290, https://doi.org/10.1515/IJNSNS.2009.10.3.273, http://www.degruyter.com/view/j/ijnsns.2009.10.3/ijnsns.2009.10.3.273/ijnsns.2009.10.3.273.xml, 2009.

Wordell-Dietrich, P., Don, A., and Helfrich, M.: Controlling factors for the stability of subsoil carbon in a Dystric Cambisol, Geoderma, 304, 40–48, https://doi.org/10.1016/j.geoderma.2016.08.023, http://dx.doi.org/10.1016/j.geoderma.2016.08.023http://linkinghub.elsevier.com/retrieve/pii/S0016706116303731, 2017.

Wotte, A., Wordell-Dietrich, P., Wacker, L., Don, A., and Rethemeyer, J.: 14 CO2 processing using an improved and robust molecular sieve cartridge, Nuclear Instruments and Methods in Physics Research Section B: Beam Interactions with Materials and Atoms, 400, 65–73, https://doi.org/10.1016/j.nimb.2017.04.019, http://www.sciencedirect.com/science/article/pii/S0168583X1730438Xhttp://linkinghub.elsevier.com/retrieve/pii/S0168583X1730438X, 2017.

Biogeosciences Discuss., https://doi.org/10.5194/bg-2019-143
Manuscript under review for journal Biogeosciences
Discussion started: 26 April 2019

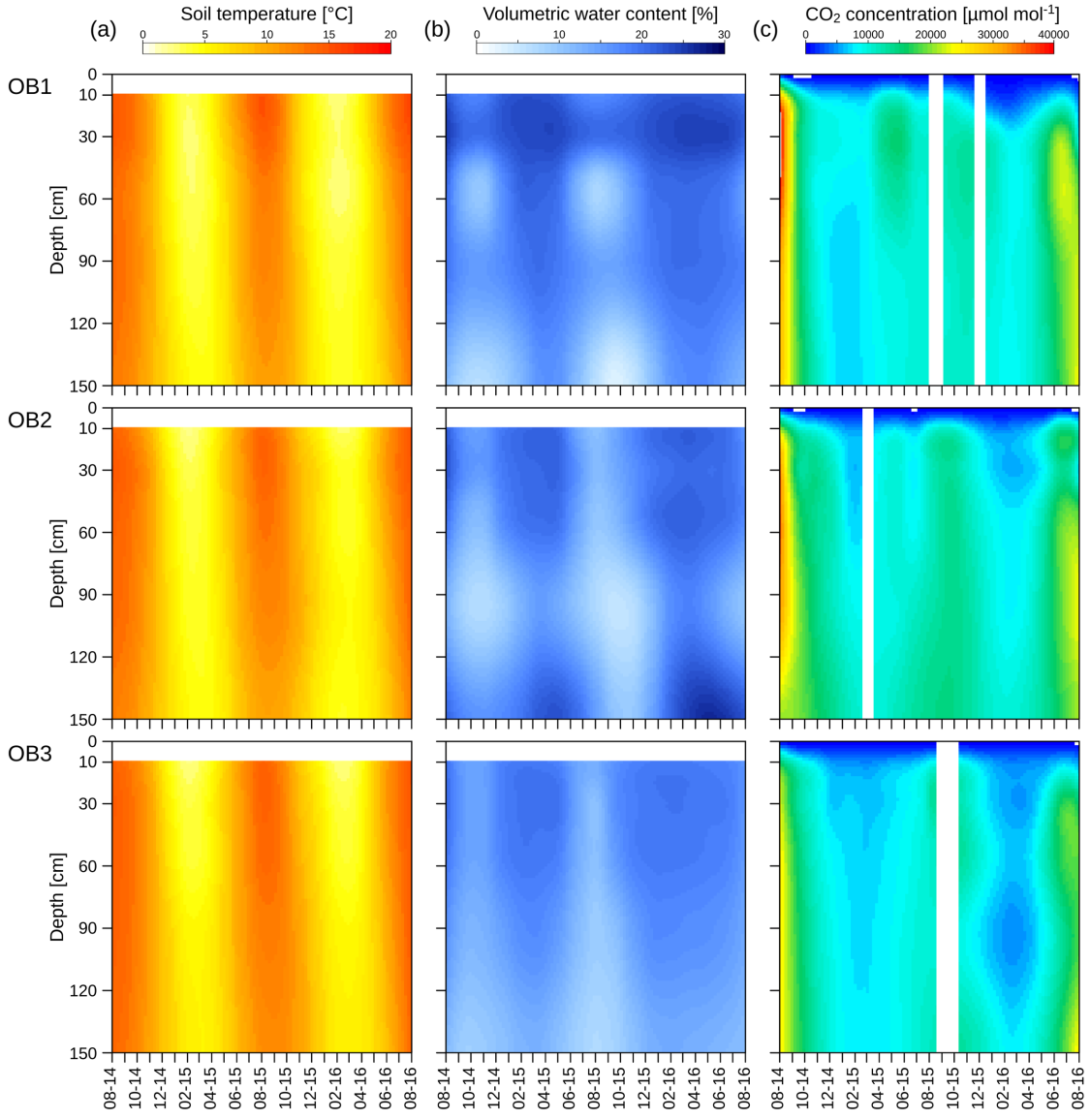

Figure 1. Soil profile measurements of temperature (a), volumetric water content (b) and CO_2 concentration for the three observatories (OB). White bars represent periods without measurements.

Biogeosciences Discuss., https://doi.org/10.5194/bg-2019-143
Manuscript under review for journal Biogeosciences
Discussion started: 26 April 2019

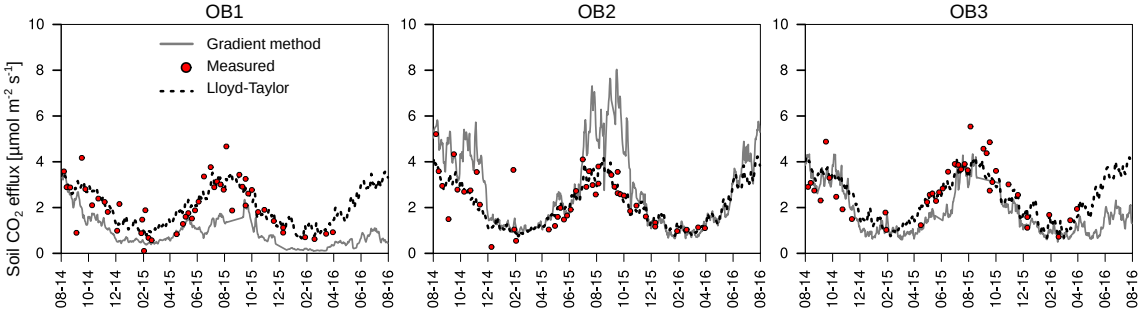

Figure 2. Mean daily soil respiration determined with the gradient method, measured with chambers and modelled with a Lloyd-Taylor function for the observatories (OB)

Biogeosciences Discuss., https://doi.org/10.5194/bg-2019-143
Manuscript under review for journal Biogeosciences
Discussion started: 26 April 2019

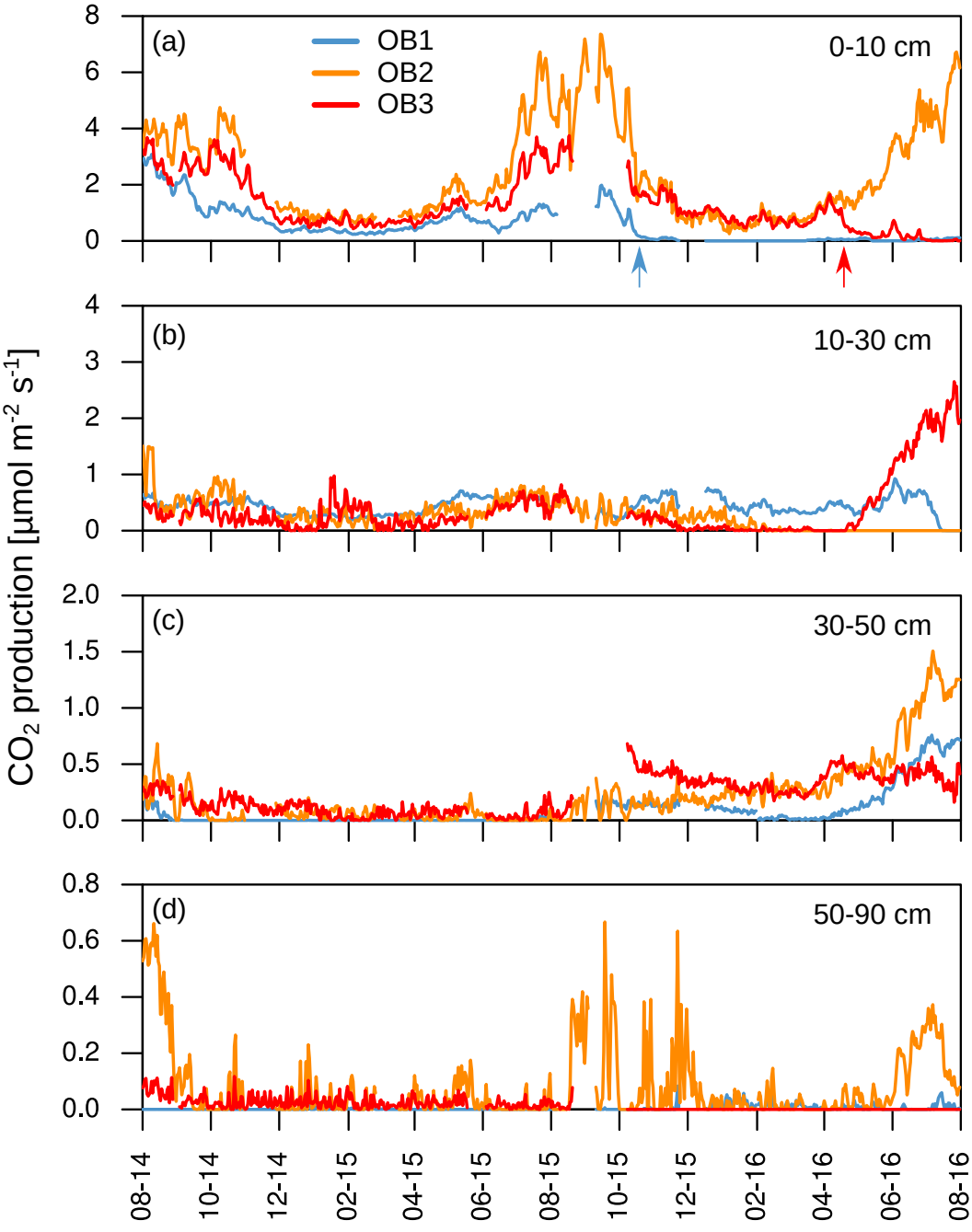

Figure 3. Daily mean CO_2 production in each soil layer (a)-(d). Arrows indicate disturbance due to bioturbation of voles in observatories (OB) 1 and 3, which created macropores and changed diffusivity.

Biogeosciences Discuss., https://doi.org/10.5194/bg-2019-143
Manuscript under review for journal Biogeosciences
Discussion started: 26 April 2019

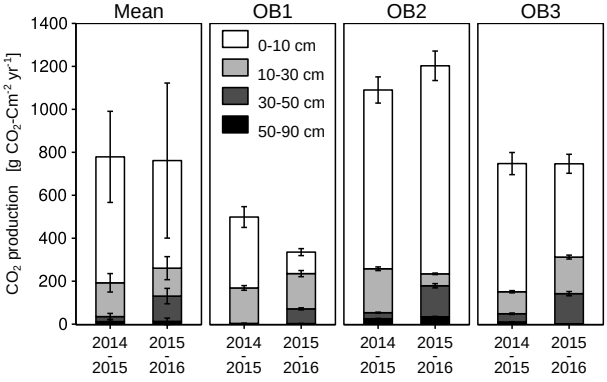

Figure 4. Cumulative CO_2 production for each soil layer, observatory (OB) and year of observation. Error bars represent standard deviation.

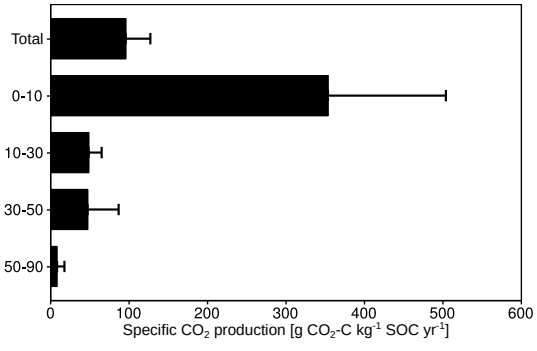

Figure 5. Mean annual specific CO_2 production for the total CO_2 efflux. Error bars represent standard deviation.

Biogeosciences Discuss., https://doi.org/10.5194/bg-2019-143
Manuscript under review for journal Biogeosciences
Discussion started: 26 April 2019

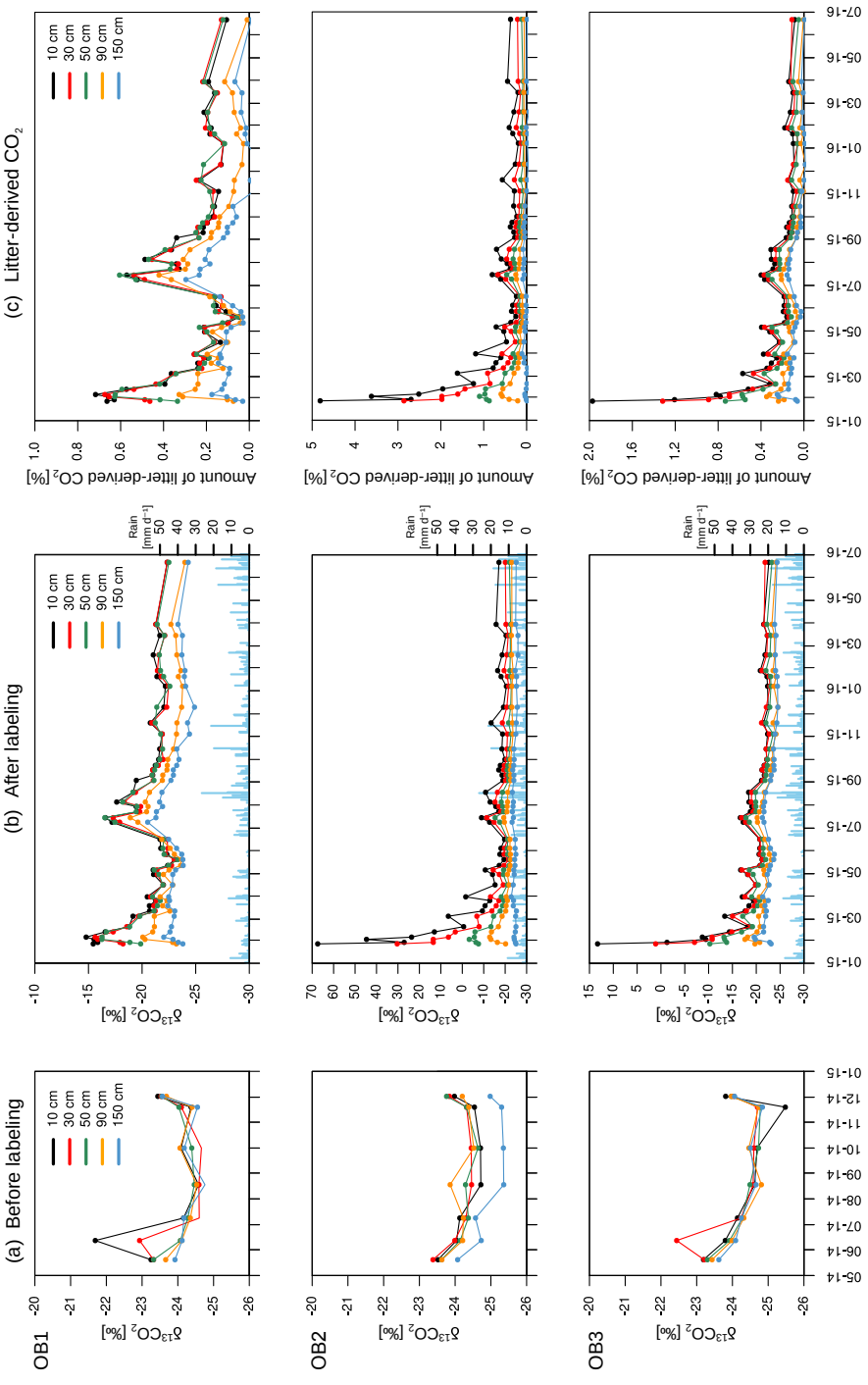

Figure 6. Isotopic signature of CO_2 at each depth and observatory (OB) before the addition of the labelled litter (a) and after labelled litter addition (b) with daily precipitation data (blue bars). The relative amount of litter-derived CO_2 on total CO2 in each depth and observatory (c). Please note the different y-axis ranges for (b) and (c).

Biogeosciences Discuss., https://doi.org/10.5194/bg-2019-143
Manuscript under review for journal Biogeosciences
Discussion started: 26 April 2019

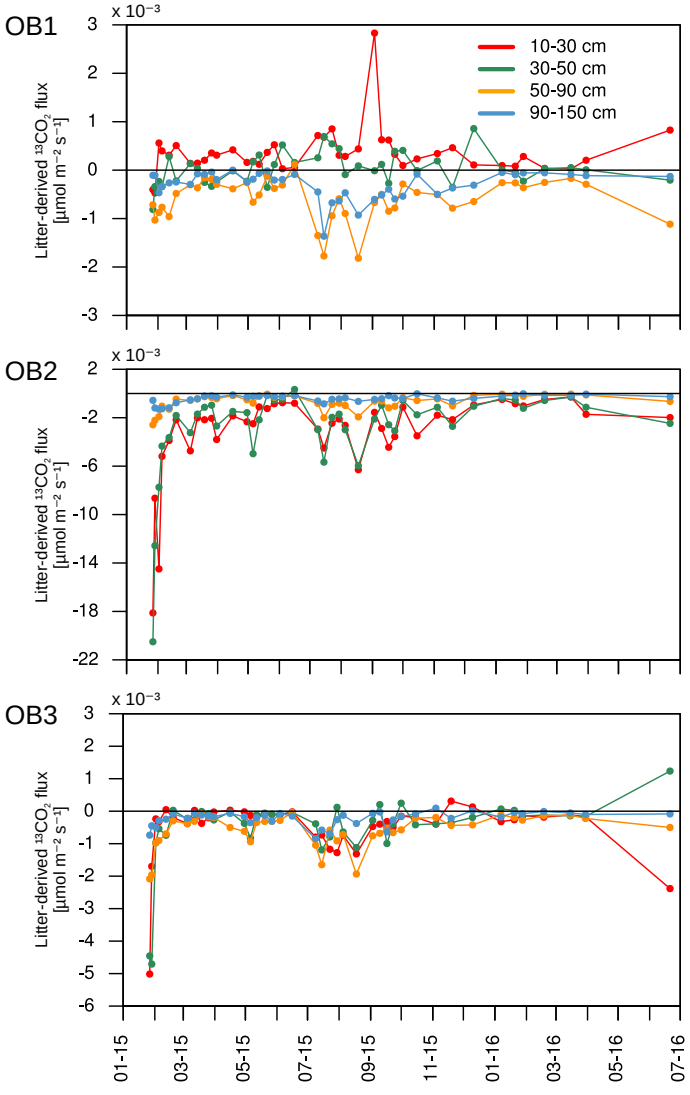

Figure 7. Litter-derived CO_2 fluxes for each observatory (OB). Positive fluxes represent mineralisation of litter-derived C. Negative fluxes represent diffusion from the layer above.

Biogeosciences Discuss., https://doi.org/10.5194/bg-2019-143
Manuscript under review for journal Biogeosciences
Discussion started: 26 April 2019

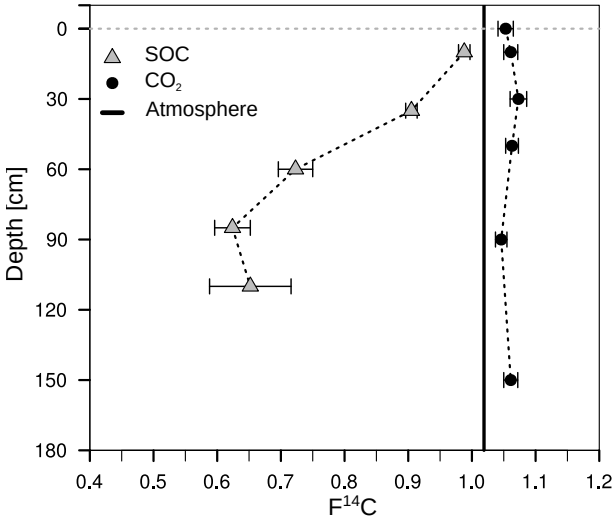

Figure 8. Mean ^{14}C concentration ($F^{14}C$) of bulk soil (grey triangles; data from Angst et al. (2016)) and CO_2 in the soil atmosphere (black dots). The solid black lines represents the annual average $F^{14}C$ value in the atmosphere from 2014 measured at the Jungfraujoch alpine research station, Switzerland (Levin and Hamer, pers. communication).

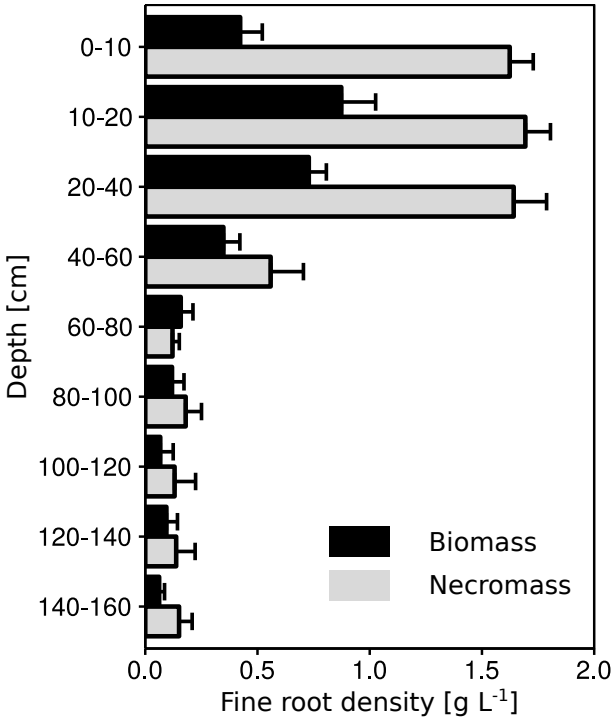

Figure 9. Mean fine root density for biomass and necromass of the subsoil observatories. Error bars represent standard error.

Biogeosciences Discuss., https://doi.org/10.5194/bg-2019-143
Manuscript under review for journal Biogeosciences
Discussion started: 26 April 2019

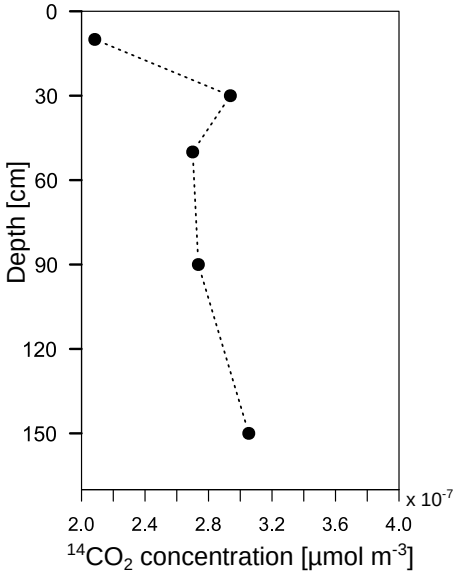

Figure 10. Soil air $^{14}CO_2$ concentration in observatory 1 from December 2014.

Biogeosciences Discuss., https://doi.org/10.5194/bg-2019-143
Manuscript under review for journal Biogeosciences
Discussion started: 26 April 2019

Table 1. Total soil respiration with and without the organic layer for the three observatories derived from soil surface measurements with linear interpolation (Chamber), modelled with a Lloyd-Taylor function and derived from the gradient method based on CO_2 measurements along the soil profile for one year. Means and standard deviations.

	Soil respiration [g C m-2 yr-1] from August 2014 to August 2015				
Observatory	without organic layer			with organic layer	
	Chamber	Llyod-Taylor	Gradient method	Chamber	Llyod-Taylor
1	699 (180)	778	447 (54)	923 (70)	990
2	804 (211)	780	1,080 (69)	860 (273)	816
3	824 (204)	916	751 (56)	1,120 (349)	980
Mean	776 (193)	825 (79)	759 (317)	967 (266)	929 (98)